Author Accepted Manuscript version of the paper by Santiago Sanchez-Acevedo, Daniel Baltensperger and Salvatore D'Arco
in 2023 IEEE Belgrade PowerTech (2023)
DOI: http://dx.doi.org/10.1109/PowerTech55446.2023.10202908

Accuracy Analysis of a Dynamic State Estimator with a Hardware in the Loop Approach

Santiago Sanchez-Acevedo
Department of energy systems
SINTEF Energy Research
Trondheim, Norway
santiago.sanchez@sintef.no

Daniel Baltensperger
Department of electrical engineering
Norwegian University of Science and Technology (NTNU)
Trondheim, Norway
daniel.s.baltensperger@ntnu.no

Salvatore D'Arco
Department of energy systems
SINTEF Energy Research
Trondheim, Norway
salvatore.darco@sintef.no

***Abstract*—State estimation is critical for the monitoring and control of power systems. The conventional approach for state estimation is based on quasi static models for the power systems and as such neglects relevant dynamic effects. These dynamic characteristics are accounted in what are referred as dynamic state estimators (DSE). Several implementations for DSEs have been proposed in literature but mostly focusing on the modelling and numerical aspects. In this paper a laboratory assessment of a DSE for estimating the internal variables of a generation plant is presented. The assessment is conducted with a Hardware in the Loop approach in a laboratory configuration that includes a PDC, real phasor measurement units (PMUs) operating with IEC 61850 sampled values and a real time model of the nordic power system. Experimental results show the behaviour and root mean square error of the estimator for a few different hardware implementations. Thus, it is assessed if the utilization of the IEC 61850 standard may have an impact on performance of the dynamic state estimation and it is quantified the effect on the accuracy.**

***Index Terms*—Dynamic state estimation, IED, PMU, cyber-physical system, wide area monitoring and control.**

I. Introduction

The future power systems are expected to pose more challenges for their operation and control due to the present trends affecting both power generation and consumption. In order to comply to commitments in reducing fossil fuels emission, power generation is gradually shifting towards a larger integration of renewables primarily by adding inverter interfaced generation units like wind turbines or photovoltaic panels. This is introducing more variability in the production due to the stochastic characteristics of these sources but also leading to a reduction of the overall power system inertia. Moreover, the decarbonization of industrial and transport sectors are contributing to an increase in the demand of electrical power leading the power systems to operate closer to their capacity limits. These expected operation challenges demand for improving the capabilities to monitor the power system and to implement faster and more effective control actions.

State estimators are implemented to monitor the power systems based on voltage and current measurements in several nodes [1]. The conventional approach is based on measurements from SCADA based Energy Management Systems (SCADA-EMS) but there are limitations in the bandwidth and in the time accuracy. Transmission system operators (TSO) have been actively improving their monitoring capabilities by adding PMUs in their power systems since these can offer a significant increase of a few orders of magnitude in the update rates and highly accurate timing due to GPS synchronization. Faster and more accurate measurements can improve the quality of the state estimation and increasing the coverage with PMUs could eventually allow also more computationally efficient implementations like linear state estimators. However, a common characteristics of the classical state estimators is that the underlying power system model is quasi static and neglects relevant dynamic characteristics. For example, the generation from power plants is modelled as active and reactive power injection.

A more recent approach in state estimations is represented by dynamic state estimators (DSE) [2] that explicitly account for dynamic characteristics of the power systems. DSE can offer several advantages in control and protection, especially in mitigating oscillatory and unstable behaviors. Dynamic state estimation has a great advantage over static state estimation, especially for security assessment. While static state estimation provides information only about the current system state, with DSE it is possible to develop computational tools that predict the short term dynamic states. This can represent a significant advantage as it allows more time for the operator to react and implement actions [3]. In addition, DSE can be used to identify and calibrate particular parameters in protection systems by testing consistency between PMU measurements and the dynamic model [2], [4].

DSE is used with the extended Kalman filter (EKF) in [5] together with trajectory sensitivity for parameters tuning. Hence, the parameters of a generator model were calibrated from deviations. Another approach where the mathematical model is compared with the measurements via DSE is the so-called Dynamic State Estimated Based Protection, also referred as (EBP). Inspired by the concept of differential protection, the basic idea is to compare the measurements with the quantities that the dynamic model of the device to be protected would provide. A systematical method to implement this is via a DSE

This paper was developed within SynchroPhasor based Automatic Real-time Control (SPARC) project, funded by the ENERGIX Program of the Research Council of Norway, under Project 280967, and the industry partners, Statnett, Fingrid, Energinet, Svenska Kraftnät, Landsnet and GE.

Author Accepted Manuscript version of the paper by Santiago Sanchez-Acevedo, Daniel Baltensperger and Salvatore D'Arco
in 2023 IEEE Belgrade PowerTech (2023)
DOI: http://dx.doi.org/10.1109/PowerTech55446.2023.10202908

[6] to compare the measurements with the mathematic model. In the field of system protection, an application was shown in [7] where a model-based and predictive out-of-step method is proposed. A two-machine equivalent is extracted 60 times per second that describes the investigated plant in the first machine and the rest of the system in the second machine. This fast model-building process relies on a dynamic state estimator. The approach predicts, based on Lyapunov's direct method, if the plant has to be disconnected or not.

The main focus in technical literature has been in the mathematical formulation and in the numerical implementation of DSEs [2], [8]–[11]. Aspects related to the possible effects on the DSEs from PMU hardware and from the communication infrastructure have been less investigated.

This paper presents an experimental assessment of a DSE for estimating the state of a generation power plant with a hardware-in-the-Loop approach (HIL). The laboratory configuration includes real PMUs and a PDC. A real time simulator runs a real time model of the european nordic power system while the DSE is executed in a client computer. Besides, IEC 61850 sampled values are used to stream data to the PMUs that generate the phasors.

The aim of the paper is to estimate the accuracy of dynamic state estimation with PMUs that receive streamed data according to the IEC 61850 sampled values standard. This work is motivated by the fact that new digital substations use IEC 61850 standard to connect the measurement devices with the processing units and relays and this also applies to PMUs. It becomes then relevant to assess if the utilization of this communication standard may have an impact on performance of the dynamic state estimation and to quantify the effect on the accuracy.

This paper is organized as follows: Section II shows the decentralized DSE modeling. Section III presents the laboratory setup developed for validating the DSE and the transmission system network used for the validation. Experimental results are presented and analysed in section IV. Finally, the conclusions are highlighted in section V.

II. Decentralized dynamic state estimator

A DSE can be implemented in a centralized or decentralized form [8]. In centralized DSE the system is assumed observable by PMUs and Kron reduction is applied to simplify the network to the nodes of the generators. On the other hand decentralized DSE uses local area PMU measurements and PMUs are located at generators buses. Hence, decentralized assumes that the node of the component under test is monitored by the local PMU and dynamic states are observable from the PMU and input measurements. Moreover, as a disadvantage centralized needs accurate knowledge of the system [2], [8]. Hence, decentralized appears as a valuable solution to estimate locally the dynamic states of generation units without adding high computational load.

A. Mathematical model of the generation plant

The DSE requires a state space dynamic model of the generation plant. This subsection describes the differential equations of the model for the generation system and the model of outputs. The differential equations of the plant follow the model $\dot{x} = F(x, u)$ described in (1)-(7) [12]. The model is written in the local synchronous frame of the generator that is oriented with the mechanical position of the shaft. The global frame is assumed to be oriented to the slack bus voltage. The states are $x^T = (\omega, E_q, E_d, \delta, E_{fd}, R_f, V_r)$. Rotational speed of the generator is defined as ω, E_d, E_q, are transient field winding voltages at d, q reference frame, δ is the angle between the global and the local frame, E_{fd} is the field voltage. R_f is the stabilizing feedback and V_r is the scaled output of the exciter. The terminal constraints are I_d, I_q and V_{in} is the magnitude of the terminal voltage. The inputs to this model are $u^T = (T_m, V_{ref})$. T_m is the mechanical torque and V_{ref} is the voltage reference of the voltage regulator system [12].

$$\dot{\omega} = \frac{\omega_s}{2H}\Big(T_m - E_d I_d - E_q I_q - (X_{qp1} - X_{dp1}) I_d I_q - D(\omega - \omega_s)\Big) \quad (1)$$

$$\dot{E}_q = \frac{1}{T_{d1}}(-E_q - (X_d - X_{dp1}) I_d + E_{fd}) \quad (2)$$

$$\dot{E}_d = \frac{1}{T_{q1}}(-E_d + (X_q - X_{qp1}) I_q) \quad (3)$$

$$\dot{\delta} = \omega - \omega_s \quad (4)$$

$$\dot{E}_{fd} = \frac{1}{Te}\Big((-K_e + S_e) E_{fd} + V_r\Big) \quad (5)$$

$$\dot{R}_f = \frac{1}{T_f}\Big(- R_f + \frac{K_f}{T_f} E_{fd}\Big) \quad (6)$$

$$\dot{V}_r = \frac{1}{T_a}\Big(K_a R_f - V_r - \frac{K_a K_f}{T_f} E_{fd} + K_a (V_{ref} - V_{in})\Big) \quad (7)$$

where, ω_s is the synchronous speed in electrical radians per second. $T_{d1}, T_{q1}, T_e, T_f, T_a$ are time constants. K_e, K_f, K_a are controller gains. Additional algebraic equations are described in (8) and (9) representing the circuit of the generator connected to the power system network. V_D and V_Q are measurements from the PMU. Hence, (8) and (9) define the outputs model z with $z = H(x, u)$. The terminal voltages at the global reference frame are V_D and V_Q and $z^T = (V_D, V_Q)$.

$$V_D = cos(\delta)(E_q - X_{dp1} I_d) + sin(\delta)(E_d + X_{qp1} I_q) \quad (8)$$

$$V_Q = -cos(\delta)(E_d + X_{qp1} I_q) + sin(\delta)(E_q - X_{dp1} I_d) \quad (9)$$

The currents measured by the PMU I_D and I_Q are in global synchronous frame. Therefore, the currents in the local synchronous frame I_d and I_q can be calculated with (10) and (11).

$$I_d = I_D sin(\delta) - cos(\delta) I_Q \quad (10)$$

$$I_q = I_D cos(\delta) + sin(\delta) I_Q \quad (11)$$

Author Accepted Manuscript version of the paper by Santiago Sanchez-Acevedo, Daniel Baltensperger and Salvatore D'Arco
in 2023 IEEE Belgrade PowerTech (2023)
DOI: http://dx.doi.org/10.1109/PowerTech55446.2023.10202908

B. Realization of the extended Kalman filter

A discrete non-linear model of the generation unit is used for the practical implementation of dynamic state estimator based on Kalman Filter. For applications with PMUs a sampling time = 20 ms is used on the discretization of the model. Therefore, (12) and (13) are used for an extended Kalman filter with process and observation noise w_k and v_k, respectively [13]. Noises covariance are Q and R for w_k and v_k, respectively. Hence, x_k and z_k are discrete variables corresponding to x and z.

$$x_k = f(x_{k-1}, u_k) + w_k \quad (12)$$
$$z_k = h(x_k, u_k) + v_k \quad (13)$$

The discrete model (12) is obtained following Euler integration of (1) to (7). $x_k \in \Re^7$. Finally, the observations model (13) is based on (8) and (9) with $z_k \in \Re^2$.

Estimated states $\hat{x}_{k|m}$ represents the estimate of x at time k given observations up to time m. The EKF has the following steps:

a) State Prediction:

$$\hat{x}_{k|k-1} = f(x_{k-1}, u_k) \quad (14)$$
$$P_{k|k-1} = F_k P_{k-1} F_k^T + Q_k \quad (15)$$

where, (14) calculates the predicted state estimate $\hat{x}_{k|k-1}$, (15) calculates the predicted covariance estimate $P_{k|k-1}$ and F_k is state transition defined by the Jacobian $\frac{\partial f}{\partial x}$ evaluated with $\hat{x}_{k-1}, u_k$.

b) State Correction:

$$\tilde{y}_k = z_k - h(\hat{x}_{k|k-1}, u_k) \quad (16)$$
$$S_k = H_k P_{k|k-1} H_k^T + R_k \quad (17)$$
$$K_k = P_{k|k-1} H_k^T S_k^{-1} \quad (18)$$
$$\hat{x}_{k|k} = \hat{x}_{k|k-1} + K_k \tilde{y}_k \quad (19)$$
$$P_k = (I - K_k H_k) P_{k|k-1} \quad (20)$$

where, $\tilde{y}$ is the measurement residual, S_k is the innovation covariance, K_k is Kalman gain, $\hat{x}_{k|k}$ is the updated state estimate, I identity matrix, $P_{k|k}$ is the updated covariance estimate and H_k is the observation matrix defined by the Jacobian $\frac{\partial h}{\partial x}$ evaluated at $\hat{x}_{k|k-1}$.

III. Laboratory Implementation

The DSE based on the extended Kalman filter is implemented for real time execution and integrated in an experimental setup to assess perfomance. The section contains a description of the laboratory configuration for HIL testing and of the grid model that is executed in real time.

A. Laboratory setup

A schematic overview of the laboratory configuration is shown in Fig. 1 highlighting the interconnection between the components including the real time simulator where the grid model is executed, the physical PMUs, the PDC and the unit where the DSE is implemented.

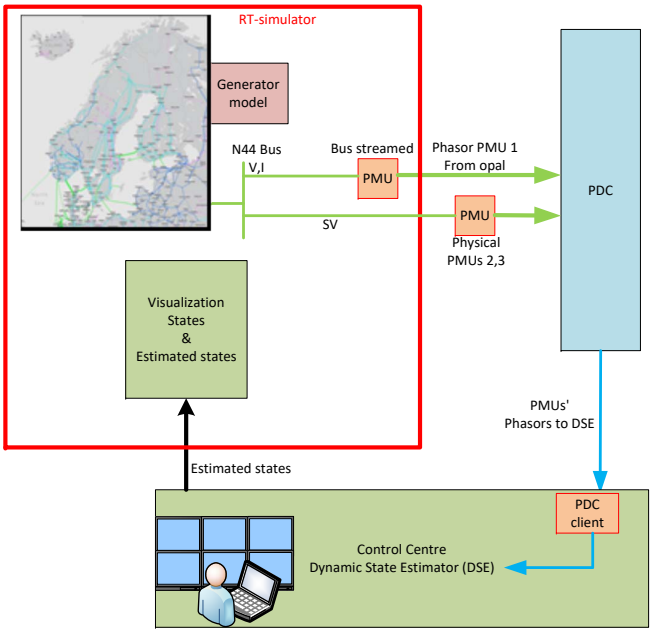

Fig. 1. Connectrions of laboratory setup. PMU 1: virtual PMU, PMU 2: ABB, PMU 3: SIEMENS.

A picture of the laboratory configuration is presented in Fig. 2 showing the real-time simulator OPAL-RT (1), the satellite synchronized network clock SEL-2488 (2), the communication switches MOXA PT-7728 used in power system substations (3), the PMU from ABB (4), the PMU from SIEMENS (5) and the configuration computers for PDC and for DSE (6).

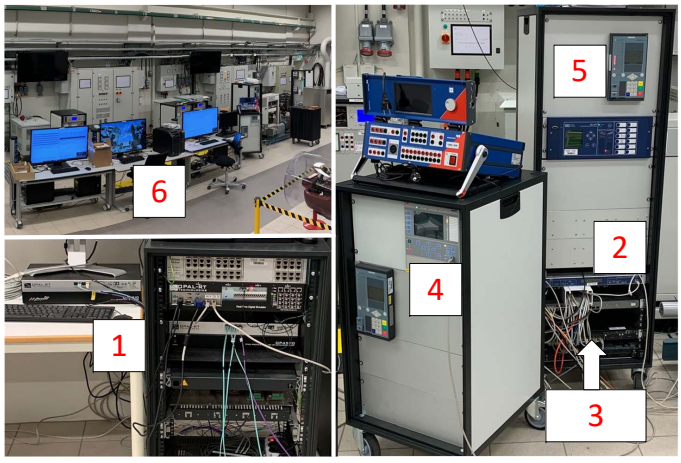

Fig. 2. View of laboratory and devices. 1: Real-time simulator, 2: GPS master clock, 3: power system substation communication switches, 4: PMU 2, 5: PMU 3, 6: Computers for PDC and Control centre DSE.

The communication between the units follows the communication protocols used on wide area monitoring, control and digital substations. The protocol C37.118 communicates with real field PMU devices or a commercial phasor data

Author Accepted Manuscript version of the paper by Santiago Sanchez-Acevedo, Daniel Baltensperger and Salvatore D'Arco
in 2023 IEEE Belgrade PowerTech (2023)
DOI: http://dx.doi.org/10.1109/PowerTech55446.2023.10202908

concentrator (PDC). Besides, the RT uses standard IEC 61850 sampled values to stream three phase sinusoidal voltages and currents to the PMU devices. This testbed uses as field devices an industrial intelligent electronic devices with PMU functionalities of class M, a grand master clock with network precision time protocol (PTP) based on GPS synchronization, power system communication switches, a configuration PC for implementing state estimator scripts or network monitoring.

The laboratory configuration contains one virtual PMU that uses directly the voltage and current phasors of the selected node of N44 where the generator is connected. Additionally, the virtual PMU is generated from the RT simulator using its C37.118 server application. Besides, Fig. 1 shows the multicast traffic based on standard IEC 61850 sampled values (SV) of the voltage and current from the node at N44. This node at N44 is the generator's connection bus. The SV packets are taken by the physical PMUs PMU 2 and PMU 3 and each device computes their phasors. Blue line is used for traffic from PDC to a PDC client at the laboratory's control centre.

B. The Nordic 44 power system model

This paper uses an openly available test model called Nordic 44 or, in short, N44. It can be downloaded online [14] and its objective is to emulate the dynamic response of the Nordic transmission system. Figure 3 shows the buses location and lines of the N44. This current version is the result of several iterations of test models representing the Nordic transmission network and has been extended over many years. There are different models between an NTNU and a KTH for the versions of the N44, both versions being extensions of the N23 model. The Norwegian version has emphasis on the Norwegian transmission system.

The N44 model has been used for stability assessments as well as market studies [14]. As the name implies, there are 44 nodes with a nominal voltage of 420 kV or 300 kV. The Norwegian part includes eight areas, Sweden four, and Finland two [15]. Additionally, there is one bus representing Denmark. The Swedish part mainly describes the large power flows from north to south where the load centers are located as well as the nuclear power plants. The Norwegian part mainly represents a large number of hydropower plants in the southwest, the power flows to the load centers around Oslo, and the transit to southern Sweden. The model includes 43 loads and 61 synchronous generators (12 in Finland, 20 in Norway and 29 in Sweden). The total power generation is of 53 GW. This is comparable to the real nordic system [16].

The N44 power system is simulated in real-time including electromechanical transient dynamics. The real-time simulator is used as a MU for the voltage and currents at the selected node of the N44.

IV. Experimental results

Three sources of PMUs have been tested in this paper as shown in Fig. 1 for node 5600 voltage and current phasors in the N44 network. PMU 1 uses the phasors directly taken

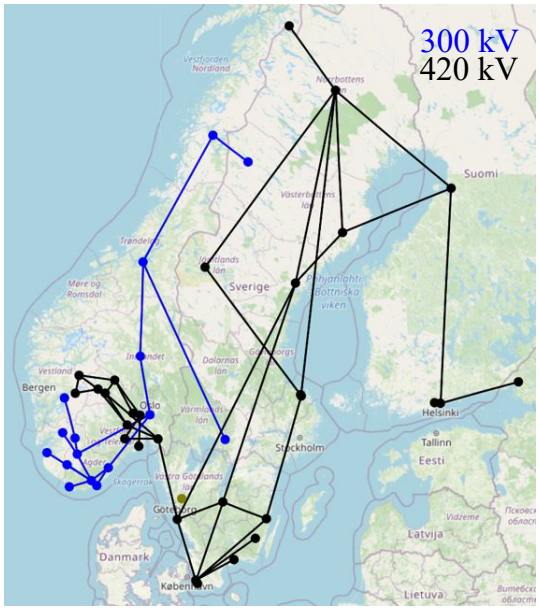

Fig. 3. Nordic 44-bus power system.

from the electromechanical RT-simulation. Therefore, PMU 1 defines the simplest and fastest PMU path to the DSE. Physical PMU 2 and PMU 3 use the sampled values of three phase voltages and currents for node 5600 in the N44. Hence, PMUs 2 and 3 calculate the phasors with the respective vendor's software.

The tests of each PMU signal for the generator at node 5600 follow the same pattern as shown in Fig. 4. The two inputs of the generation unit have been changed with the aim of exciting the different dynamic states. Initially at t = 0 s a step was applied on the mechanical torque (T_m) with an increment of 0.1 p.u (see Fig. 4 top). The step of T_m produces a transient that excites the performance of the dynamic state estimation with the three different PMUs. The step was removed at $t = 32.62$ s. After step of T_m a step on the generator's reference voltage (V_{ref}) was applied at t = 72.62 s and it was removed at $t = 92.62$ s. Moreover, Fig. 4 shows the rectangular form of voltage V_D, V_Q and current I_D, I_Q phasors of the electromechanical RT-simulation at node 5600 in the N44. It is shown the current changes from $t = 0$ s produced by the T_m step and at $t = 72.62$ s I_Q and I_D increase the magnitudes as a result of the change of V_{ref}. The RT-simulator is PMU 1 defined with sub-index $opal$. PMU 2 is defined with sub-index abb. Finally, PMU 3 is defined with sub-index sie. True generator states are denoted with $x \in \{V_r, R_f, E_d, E_q, \delta, E_f, \omega\}$ and estimated values are denoted with $\hat{x}$.

The behaviour of PMU 1, 2 and 3 for estimating states V_r and R_f are shown in Fig. 4 bottom. States V_r and R_f are sensitive to step change of V_{ref}. Root mean square errors (RMSE) for the estimation of V_r and R_f are shown in Table I. PMU 1 generates the lowest RMSE fro estimation of V_r and R_f. Figure 5 shows the estimation for the states E_q, E_d,

Author Accepted Manuscript version of the paper by Santiago Sanchez-Acevedo, Daniel Baltensperger and Salvatore D'Arco
in 2023 IEEE Belgrade PowerTech (2023)
DOI: http://dx.doi.org/10.1109/PowerTech55446.2023.10202908

δ, E_f and ω. State E_q is sensitive to a step on V_{ref}. Fig. 5 top shows the behaviour of estimation E_q with the different PMUs. Estimations for E_q show a smooth transition. Besides, the RMSE errors for this state are very close for all the PMUs as shown in Table I. PMU 3 estimation shows the lowest RMSE for E_q. E_d is a state that stays close to zero as shown in Fig. 5. Fig. 5 shows the estimation of δ. State δ is highly excited by T_m changes. Figure 5 and Table I show the largest estimation error and RMSE of δ with PMU 1. Estimations of E_{fd} are shown in Fig. 5, the behaviour of estimations are similar to E_q. RMSE are similar for PMU 2 and PMU 3. PMU 1 produces the lowest RMSE of E_{fd}. Finally, Fig. 5 bottom shows the estimation of ω. Changes of T_m excites oscillation of ω. RMSEs from the three different PMUs is very similar (see Table I). However, PMU 1 produces the lowest RMSE. Finally, results present a maximum RMSE of 1.65 % on states with p.u. values and a maximum RMSE 0.0141 rad of state δ.

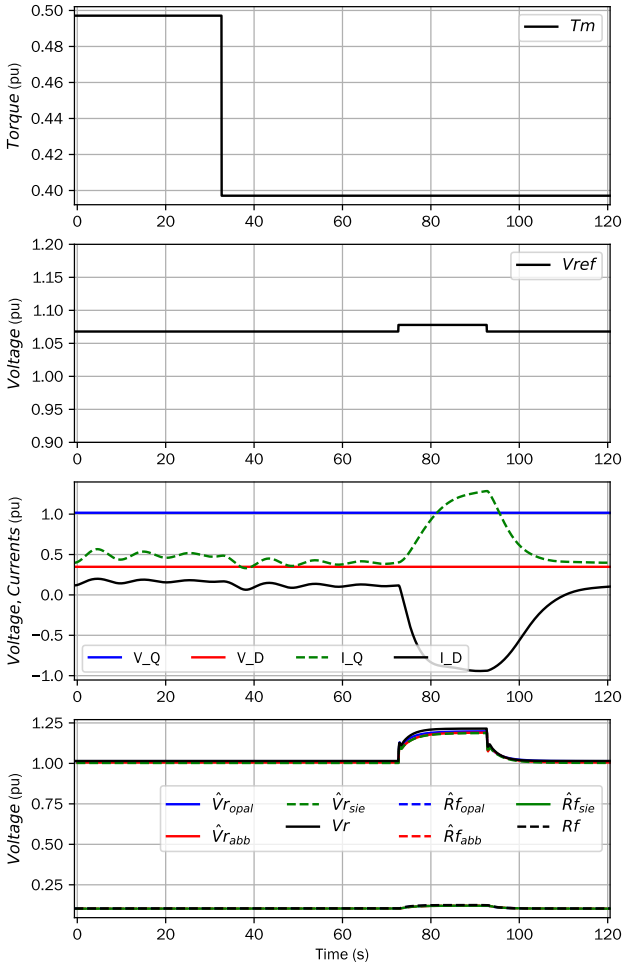

Fig. 4. DSE inputs T_m, V_{ref}, states V_r and R_f.

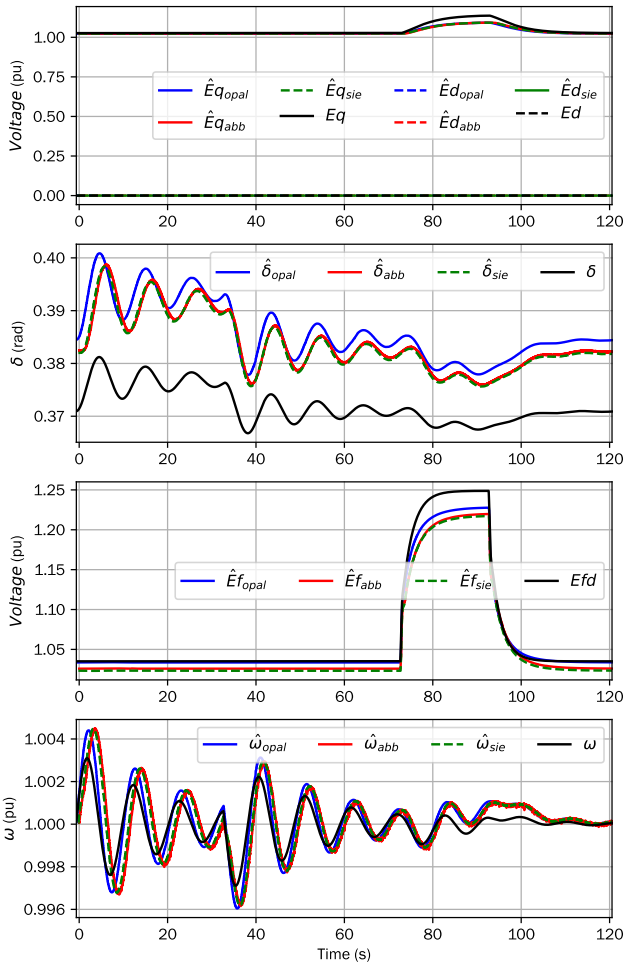

Fig. 5. DSE of states E_q, E_d, δ, E_{fd} and ω.

TABLE I
ROOT MEAN SQUARE ERROR FOR DSE WITH PMUS

State	PMU type		
	PMU 1: opal	***PMU 2: abb***	***PMU 3: sie***
V_r	0.00122534	0.0016823	0.00167742
R_f	0.007255	0.0138511	0.01557030
E_q	0.016427	0.01595	0.01469
E_d	3.5130×10^{-5}	3.7217×10^{-5}	3.1254×10^{-5}
δ	0.014149	0.012066	0.011597
E_{fd}	0.00902104	0.0152296	0.0164983
ω	0.00052668	0.0008533	0.00071267

Author Accepted Manuscript version of the paper by Santiago Sanchez-Acevedo, Daniel Baltensperger and Salvatore D'Arco
in 2023 IEEE Belgrade PowerTech (2023)
DOI: http://dx.doi.org/10.1109/PowerTech55446.2023.10202908

V. Conclusions

The paper has assessed the performance of a dynamic state estimator for estimating the state of a generation power plant connect to a transmission grid. The assessment is conducting on an experimental configuration with an hardware-in-the-loop approach. It is shown the performance of an extended Kalman filter for a dynamic state estimator with multiple PMU sources. The first PMU (PMU 1) source gives the ideal path without any recalculation of the phasors by the PMU devices. PMU 2 and PMU 3 used a realistic environment with IEC 61850 sampled values applied to get three phase sinusoidal current and voltages. Hence, PMU 2 and PMU 3 calculate the phasors and send them to the system operator's PDC. Estimation with physical devices showed good performance based on the analysis of results of section IV. RMSE of states E_d and δ are better with physical PMUs than RMSE with the ideal PMU path. The estimation of ω shows comparable RMSE for all the PMUs. Estimated values followed the profile of the real states with a small offset, with a maximum RMSE of 1.65 $\%$ on states with p.u. values and maximum RMSE 0.0141 rad for δ. Hence, the environment produces reliable values that can be used on applications like protection systems. Moreover, it has been obtained a degree of accuracy for DSE in new digital substations that comply with IEC 61850 standard.

References

[1] J. Zhao, "Power system dynamic state estimation considering measurement correlations," *IEEE Transactions on Energy Conversion*, vol. 32, no. 4, pp. 1630–1632, 2017.

[2] J. Zhao, A. Gómez-Expósito, M. Netto, L. Mili, A. Abur, V. Terzija, I. Kamwa, B. Pal, A. K. Singh, J. Qi, Z. Huang, and A. P. S. Meliopoulos, "Power system dynamic state estimation: Motivations, definitions, methodologies, and future work," *IEEE Transactions on Power Systems*, vol. 34, no. 4, pp. 3188–3198, 2019.

[3] N. R. Shivakumar and A. Jain, "A review of power system dynamic state estimation techniques," in *2008 Joint International Conference on Power System Technology and IEEE Power India Conference*, 2008, pp. 1–6.

[4] E. Farantatos, R. Huang, G. J. Cokkinides, and A. P. Meliopoulos, "A predictive generator out-of-step protection and transient stability monitoring scheme enabled by a distributed dynamic state estimator," *IEEE Transactions on Power Delivery*, vol. 31, no. 4, pp. 1826–1835, 2016.

[5] Z. Huang, P. Du, D. Kosterev, and S. Yang, "Generator dynamic model validation and parameter calibration using phasor measurements at the point of connection," *IEEE Transactions on Power Systems*, vol. 28, no. 2, pp. 1939–1949, 2013.

[6] A. P. S. Meliopoulos, G. J. Cokkinides, P. Myrda, Y. Liu, R. Fan, L. Sun, R. Huang, and Z. Tan, "Dynamic state estimation-based protection: Status and promise," *IEEE Transactions on Power Delivery*, vol. 32, no. 1, pp. 320–330, 2017.

[7] E. Farantatos, R. Huang, G. J. Cokkinides, and A. P. Meliopoulos, "A predictive generator out-of-step protection and transient stability monitoring scheme enabled by a distributed dynamic state estimator," *IEEE Transactions on Power Delivery*, vol. 31, no. 4, pp. 1826–1835, 2016.

[8] E. Ghahremani and I. Kamwa, "Local and wide-area pmu-based decentralized dynamic state estimation in multi-machine power systems," *IEEE Transactions on Power Systems*, vol. 31, no. 1, pp. 547–562, 2016.

[9] J. Zhao, "Dynamic state estimation with model uncertainties using h_∞ extended kalman filter," *IEEE Transactions on Power Systems*, vol. 33, no. 1, pp. 1099–1100, 2018.

[10] J. Zhao and L. Mili, "Robust unscented kalman filter for power system dynamic state estimation with unknown noise statistics," *IEEE Transactions on Smart Grid*, vol. 10, no. 2, pp. 1215–1224, 2019.

[11] ——, "A robust generalized-maximum likelihood unscented kalman filter for power system dynamic state estimation," *IEEE Journal of Selected Topics in Signal Processing*, vol. 12, no. 4, pp. 578–592, 2018.

[12] P. W. Sauer and M. A. Pai, *Power system dynamic and stability*. The University of Illinois, 1997.

[13] S. Haykin, *Adaptive Filter Theory*, 3rd ed. Prentice-Hall Inc., 1996.

[14] S. H. Jakobsen, L. Kalemba, and E. H. Solvang, "The nordic 44 test network," 2018. [Online]. Available: https://figshare.com/projects/Nordic_44/57905

[15] S. M. Hamre, "Inertia and fcr in the present and future nordic power system," Master's thesis, Norwegian University of Science and Technology - NTNU, 2015.

[16] S. D'Arco, T. D. Duong, and J. Are Suul, "P-hil evaluation of virtual inertia support to the nordic power system by an hvdc terminal," in *2020 IEEE PES Innovative Smart Grid Technologies Europe (ISGT-Europe)*, 2020, pp. 176–180.